Characterisation of a spinning pipe gas lens using a Shack–Hartmann wavefront sensor

Cosmas Mafusire*[a,b], Andrew Forbes[a,b], Glen Snedden[c] , and Max M. Michaelis[b]
[a]CSIR National Laser Centre, PO Box 395, Pretoria 0001, South Africa
[b]School of Physics, University of Kwazulu-Natal, Private Bag X54001, Durban 4000, South Africa
[c]CSIR Defence Peace Safety and Security, PO Box 395, Pretoria 0001, South Africa

ABSTRACT

A heated horizontal spinning pipe causes gases inside it to assume dynamics resulting in a graded index lens – a spinning pipe gas lens (SPGL). A CFD model is presented which shows that gas exchanges of the SPGL with the surroundings resulting in a near parabolic density distribution inside the pipe created by the combination of velocity and thermal boundary layers. Fluid dynamic instabilities near the wall of the pipe are thought to have an deleterious effect on the quality of the beam and its wavefront. Measurements of the wavefront of a propagating laser beam shows strong defocus and tilt as well as higher order aberrations, thereby reducing the beam quality factor (M^2) of the output beam. Results are presented as a function of pipe wall temperature and pipe rotation speed.

Keywords: Spinning pipe gas lens, Zernike polynomials, GRIN lens, optical wavefront

1. INTRODUCTION

The device discussed in this paper is a heated steel pipe and made to rotate (or spin) horizontally about its axis, thus forming a graded refractive index profile across the diameter of the pipe. Under certain conditions this profile leads to wave guiding, and with judicious choice of pipe length, an output beam that is converging in space can be obtained. When this happens, the system is seen to act as a lens, and is referred to as a spinning pipe gas lens (SPGL). Interest in this type of gas lens began in the early 1960s when scientists at Bell laboratories used gas lenses they had developed as waveguides[1–5]. The early gas lenses did not guide beams by being spun but rather by a laminar flow of gas that would be injected axially into a heated, stationary pipe and exhausted radially[2–7]. The idea of rotating a heated metal pipe was introduced in 1975 by Martynenko[8] where it was shown both theoretically and experimentally that lens, overcame the asymmetric nature of the temperature field and removed aberrations caused by free convection.

However, most of the studies carried out then and since have concentrated on the lensing aspect alone; for example, to focus intense laser beams for the drilling of holes in metal sheets, and as telescope objectives[9-12]. These studies did not consider the effect the SPGL had on the quality and wavefront of the propagating laser beam.

This paper concentrates on the use of a Shack–Hartmann wavefront sensor to simultaneously measure both wavefront deformation caused by the SPGL and deterioration in beam quality. Section 2 discusses some established theories and experimental results about the SPGL and how these can be related to basic knowledge about wavefront deformation and the beam quality factor, M^2. Section 3 gives an introduction to Zernike coefficients. Section 4 discusses a Computational Fluid Dynamics (CFD) model of the random mixing of hot and cold gases in the SPGL which will play an important part in analysis of results. Section 5 shows a description of the experiment and a discussion of results thus acquired.

2. SPINNING PIPE GAS LENS

The SPGL can be regarded as a graded refractive index (GRIN) lens. Under ideal conditions its refractive index distribution has been shown to approximate a parabolic profile of the form[11,13–15]:

$$n(r) = n_o - \tfrac{1}{2} a r^2 , \qquad (1)$$

* cmafusire@csir.co.za; phone +27 12 841 3900; fax +27 12 841 3152

Laser Beam Shaping VIII, edited by Fred M. Dickey, David L. Shealy,
Proc. of SPIE Vol. 6663, 66630H, (2007)
0277-786X/07/$18 · doi: 10.1117/12.734110

where r is the radial distance from the axis, a is a radial refractive index parameter which is a measure of the power of the SPGL and n_o is the refractive index along the axis. The parameter a implies that the SPGL focuses a beam $\sqrt{a}$ times per unit distance. This means it is possible to get either a diverging, collimated or converging laser beam after passing it through an SPGL. To get a converging or focused beam, the GRIN medium inside must be in the process of focusing the beam on exit. Under these conditions, it is possible to measure its focal length.

In a previous study[15], the SPGL's focal length variation with rotation speed at selected temperatures was investigated experimentally; the results are reviewed in Figure 1 for convenience. The data clearly demonstrates the inverse relationship between the pipe rotation speed and the resulting focal length. An empirical formula for the focal length f was deduced as:

$$f(\omega, T) = 8.62 \times 10^{13} \omega^{-1.6} T^{-4.5}, \quad (2)$$

T represents the SPGL wall temperature in Kelvin and ω is its rotation speed in Hertz. The graph also shows that for higher temperature, the SPGL focal length becomes smaller for a given rotation speed. The same focal length trend is noted when increasing the rotation rate at constant temperature.

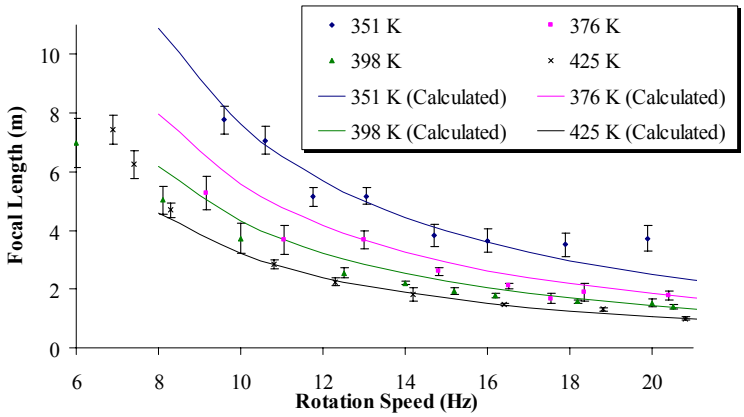

Figure 1: A graph showing the inverse relationship between focal length and rotation speed at selected temperatures

However, the above information does not indicate anything about the changes to the wavefront of the beam due to the SPGL. Also, it has been suggested that in some cases the refractive index profile is not parabolic, and may even have a flat central region[10,14,16]. Such hypothesis may only be tested by considering the wavefront of the beam passing through the SPGL. To get this information, the focus should be on the wavefront itself. This means that there is need to look at the SPGL from the point of view of the gas mixing, laser beam wavefront deformation and the corresponding changes to the beam quality.

The rotation of the pipe, together with the heated walls, result in a stable region (in terms of density changes) in the central region of the pipe, which becomes more unstable nearer the walls of the pipe due to the combination of the rotational and longitudinal velocity boundary layers which are small in relation to the pipe diameter. Overlaid with these velocity boundary layers is a thermal boundary layer extending to the centre of the pipe. If a laser beam is propagated in such conditions, it is reasonable to expect that the unstable regions would result in refractive index variations with a concomitant increase in randomness in the laser beam's wavefront. Such a scenario would manifest itself not only in high order aberrations, but also in an increase in the laser beam quality factor, M^2. A convenient manner to describe aberrations of low and high order is the Zernike basis set, considered in the following section.

3. ZERNIKE POLYNOMIALS

The Zernike polynomials are a set of orthogonal polynomials that arise in the expansion of a wavefront function for optical systems with circular pupils[17]. The expansion of an arbitrary function $\Phi(\rho,\theta)$ where $\rho \in [0,1]$ and $\theta \in [0,2\pi]$, in an infinite series of these polynomials will be complete. The circle polynomials of Zernike have the form of complex angular function modulated by a real radial polynomial:

$$Z_n^m(\rho,\theta) = R_n^m(\rho)[\cos(m\theta) + i\sin(m\theta)], \tag{3}$$

where $n \geq m$, $n \geq 0$ and $n - m = \text{even}$. It can be shown that the radial function, obeys an orthogonality relation, and is given by:

$$R_n^m(\rho) = \sum_{k=0}^{\frac{n-m}{2}} \frac{(-1)^k (n-k)!}{k!(\frac{n+m}{2}-k)!(\frac{n-m}{2}-k)!} \rho^{n-2k}, \tag{4}$$

This function is normalised such that:

$$R_n^m(1) = 1, \tag{5}$$

By definition, $R_n^m = 0$ when $n - m \neq \text{even}$. We can construct two real functions U_n^m and V_n^m such that equation (1) can be written as:

$$Z_n^m(\rho,\theta) = U_n^m(\rho,\theta) + iV_n^m(\rho,\theta), \tag{6}$$

It has been shown that any function $\Phi(\rho,\theta)$ can be written in terms of U_n^m and V_n^m such that:

$$\Phi(\rho,\theta) = \sum_{n=0}^{\infty}\sum_{m=0}^{n}[A_n^m U_n^m(\rho,\theta) + B_n^m V_n^m(\rho,\theta)], \tag{7}$$

where the Zernike coefficients A_n^m and B_n^m are given by:

$$A_n^m = K(m)\frac{n+1}{\pi}\int_0^{2\pi}\int_0^1 \Phi(\rho,\theta)U_n^m(\rho,\theta)\rho d\rho d\theta, \tag{8}$$

$$B_n^m = K(m)\frac{n+1}{\pi}\int_0^{2\pi}\int_0^1 \Phi(\rho,\theta)V_n^m(\rho,\theta)\rho d\rho d\theta, \tag{9}$$

where

$$K(m) = \begin{cases} 2, & m \neq 0 \\ 1, & m = 0 \end{cases}$$

The measured change in phase, $\Phi(\rho,\theta)$, is used to determine the aberration coefficients A_n^m and B_n^m from (8) and (9) respectively. With these coefficients we can then express $\Phi(\rho,\theta)$ as an expansion of Zernike coefficients as in (7). The first ten coefficients are shown in Table 1. Note that the piston term has been excluded as it affects the entire beam uniformly.

The above formulation can be used calculate the aberrations due to a lens of focal length f:

$$\Phi(\rho) = -\frac{ka^2\rho^2}{2f}, \tag{10}$$

where a is the radius of the pupil, ρ is its normalised radius and k is the wave constant. Substituting (10) in (8) and (9) yields:

$$A_2^0 = -\frac{ka^2}{4f}, \tag{11}$$

with all the other Zernike coefficients, except piston, being equal to zero. A similar calculation for the SPGL using (1) also identifies defocus as the only aberration caused by the SPGL.

Table 1 The first ten aberrations with piston ignored according to the model above

	Aberration Coefficient	Polar Coordinates	Aberration Description
1	B_1^1	$\rho \sin\theta$	Tilt about y–axis
2	A_1^1	$\rho \cos\theta$	Tilt about x–axis
3	A_2^0	$2\rho^2-1$	Defocus
4	A_2^2	$\rho^2 \cos2\theta$	Primary stigmatism with 0 or 90º axis
5	B_2^2	$\rho^2 \sin2\theta$	Primary astigmatism with ± 45º axis
6	A_3^1	$(3\rho^3-2) \cos\theta$	Primary coma along x–axis
7	B_3^1	$(3\rho^3-2) \sin\theta$	Primary coma along y–axis
8	A_3^3	$\rho^3 \cos3\theta$	Triangular astigmatism with base along y–axis
9	B_3^3	$\rho^3 \sin3\theta$	Triangular astigmatism with base along x–axis
10	A_4^0	$6\rho^4-6\rho^2+1$	Primary spherical aberration

4. THE COMPUTATIONAL FLUID DYNAMICS MODEL

Computational Fluid Dynamics (CFD) simulations of a simplified test set up were performed using the commercial CFD code, STAR–CD. Assumptions included the removal of the bearing blocks and other 3 dimensional geometry features that would complicate the geometric model. The tube, however, is accurately reproduced with the further assumption that the bearing blocks act as a heat sink and hence the tube ends are unheated. A fully transient solution is presented in which the tube is spun up from a heated steady-state buoyancy driven solution and held at speed until steady state is reached. Turbulence is modelled using the k–ε model[18].

The model shows that there is a very slow velocity field near the ends of the pipe which exchanges gas with the surroundings by drawing cold air in near the centre of the pipe, and exhausting hot air out near the edges of the pipe. Towards the middle of the pipe the flow is very uniform but very slow, with a boundary layer close to the wall of the pipe (estimated at a tenth of the pipe diameter). This is illustrated in Figure 2 where one frame of the transient simulation is shown. This longitudinal velocity boundary layer interacts with the rotational velocity boundary layer. The pipe wall is rotating at roughly twice the speed of the longitudinal velocity at the wall, and the interaction gives rise to an unstable region with helical–like flow.

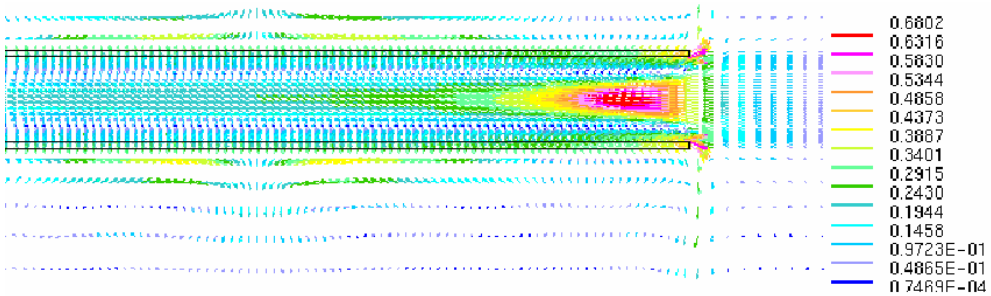

Figure 2: Velocity field showing net flow inwards at the centre of the pipe and net flow outwards near the wall of the pipe. The gradient of the field decreases as one moves towards the middle of the pipe, showing that this exchange is mostly due to effects at the pipe ends.

Because of the slow flow, the thermal boundary layer is able to extend to the centre of the pipe in the radial direction over the entire heated section of the pipe. This large boundary layer is what gives rise to the density profile across the pipe diameter, which is mostly stable with a small unstable region near the pipe wall.

When the pipe is not rotated, the heated pipe's density gradient is driven by convection currents. As the rotation begins,

the density profile adopts a more radially symmetric profile which becomes more defined as the rotation speed increases. The CFD results illustrating the initial and transient density profiles are shown in Figures 3 (a) and (b) respectively..

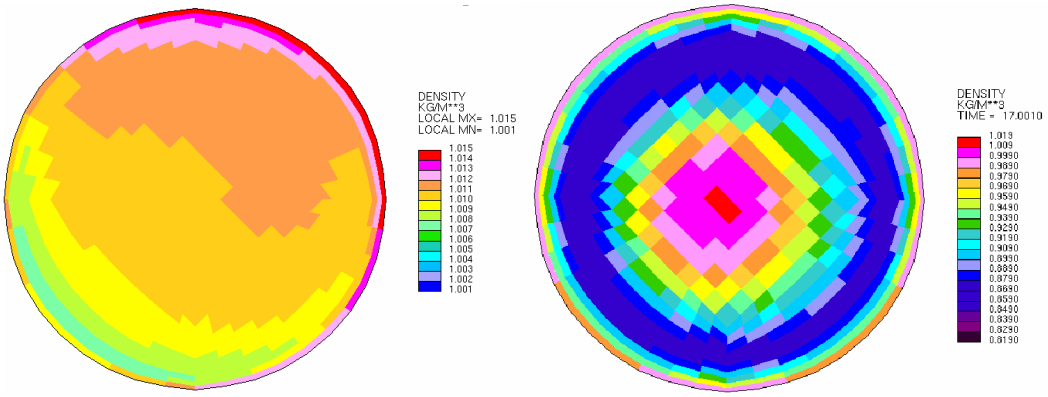

(a) (b)

Figure 3: Cross–sectional density profile showing (a) initial state (b) transient state.

5. WAVEFRONT SENSOR RESULTS

A laser beam from a HeNe source was first attenuated by neutral density filters, expanded by an afocal telescope then steered into an SPGL by two flat mirrors. The beam was then incident on a Shack-Hartmann sensor from which the frames were transferred to a computer for processing. A beam was passed through the pipe without any rotation or heating. Measurements from this beam were recorded as reference. The pipe was heated to temperatures 354, 375, 402 and 429 K. At each of the four temperatures and selected rotation speeds, at least 15 sets of readings were acquired. Each set consisted of the first ten Zernike coefficients and M^2. For each Zernike coefficient and M^2, the 15 values were averaged. This experimental set-up used is shown in Figure 4.

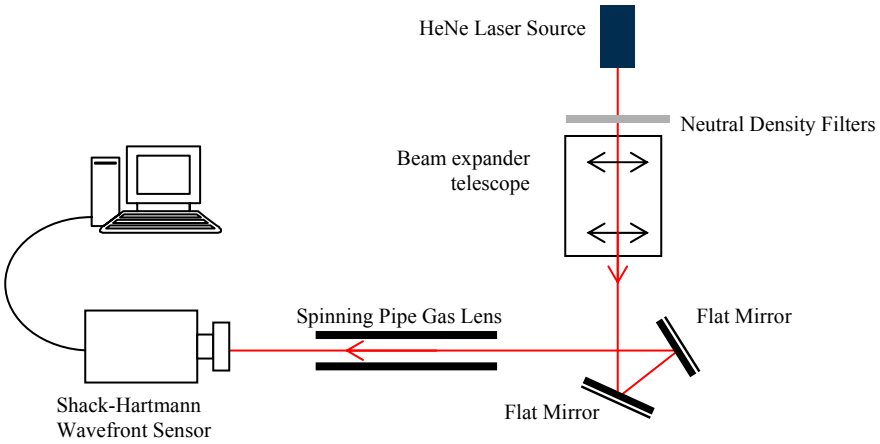

Figure 4: The experimental set-up for the measuring the aberrations caused by the spinning pipe gas lens

Table 2 shows Zernike coefficients for the SPGL with wall temperature set at 375 K. This table is representative of the trends observed at other temperatures and is used here as an example only. Tilt about the *x*–axis showed the most change as the rotation speed increased, followed by the expected defocus. As the aberrations increase in order, so their magnitude decreased. Although the coefficients of the higher order aberrations are small, they are nevertheless not negligible, as will be shown later.

Table 2 Results for the first ten Zernike coefficients as the SPGL rotation speed is increased with the SPGL's temperature set at 375 K

Zernike Term		Rotation Speed (Hz)									
		0	1.5	2.4	4.7	5.9	8.2	10.1	12.5	15.0	16.4
B_1^1	Aberration Coeffs (waves)	0	-0.420	-0.332	-0.161	-0.103	-0.133	-0.491	-0.241	-0.023	0.042
A_1^1		0	2.206	2.442	2.437	2.854	3.558	3.930	4.263	4.602	4.967
A_2^0		0	-0.086	-0.073	-0.047	-0.053	-0.059	-0.105	-0.077	-0.080	-0.005
A_2^2		0	-0.241	-0.343	-0.446	-0.560	-0.743	-0.899	-1.025	-1.235	-1.216
B_2^2		0	0.018	0.023	0.021	0.035	0.053	0.044	0.069	0.085	0.117
A_3^1		0	-0.001	0.000	0.007	0.007	0.001	0.004	-0.004	-0.010	0.003
B_3^1		0	-0.010	-0.012	-0.018	-0.019	-0.008	0.011	0.005	0.003	-0.017
A_3^3		0	0.001	-0.005	-0.013	-0.020	-0.030	-0.035	-0.048	-0.072	-0.079
B_3^3		0	0.005	0.004	0.009	0.004	0.000	-0.011	-0.015	-0.019	-0.017
A_4^0		0	0.021	0.011	0.013	0.011	0.008	0.008	0.007	0.006	0.009

Figure 5 considers the change in tilt as a function of rotation speed and temperature. Clearly the magnitude of the aberration increases with rotation speed and temperature. That this is the major term is a surprising outcome of this study, as the SPGL as described by (10) would only contribute to the defocus term. We speculate that tilt is due to either asymmetric heating of the pipe and/or the contributions from the unstable regions within the pipe.

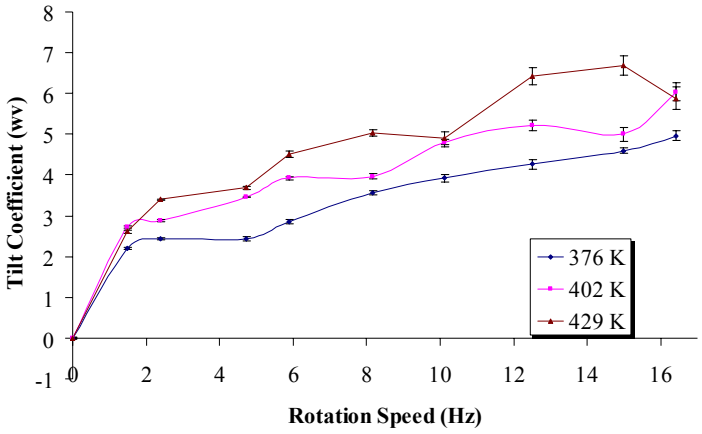

Figure 5: Variation of tilt (A_1^1) with SPGL rotation speed at selected temperatures

The change in defocus is shown graphically in Figure 6. The results show an expected general trend that lensing becomes stronger at increased rotation rates. To examine this further, the measured wavefront changes were converted to corresponding effective focal lengths, and then plotted against focal length acquired using the previously found empirical relation (Eq. (2)). The result is shown in Figure 7. Although the relationships are linear, the wavefront sensor appears to be under estimating the focal length by approximately 20–30%, as calculated from the slopes of the trends. At present the reason for this is not well understood, and requires further investigation.

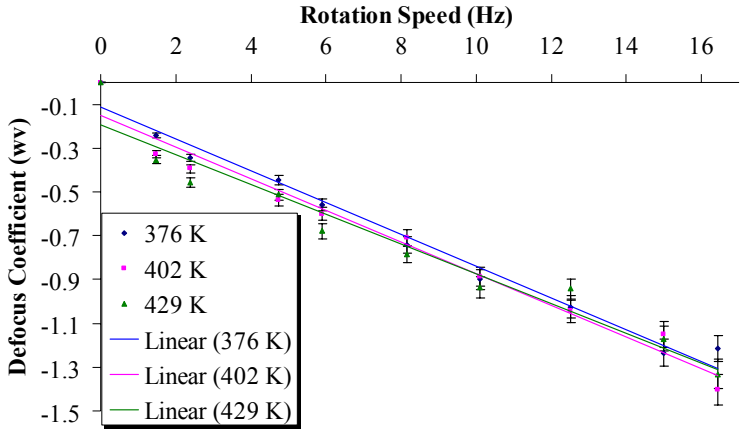

Figure 6: Variation of defocus (A_2^0) with SPGL rotation speed together with calculated graphs at selected temperatures

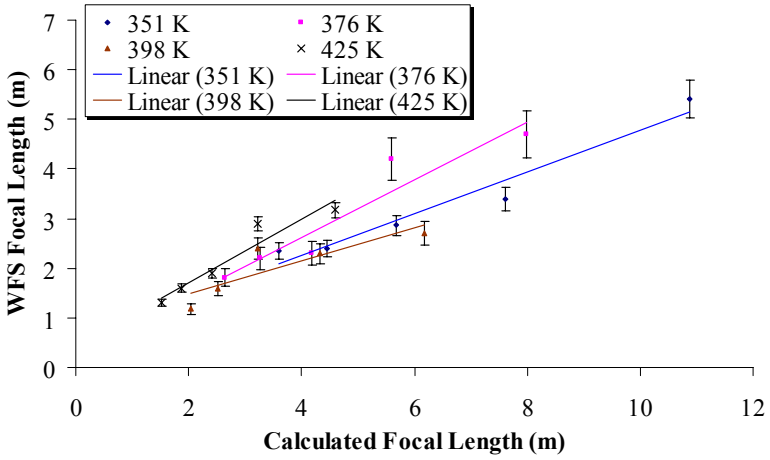

Figure 7: Graphs relating calculated focal length with wavefront sensor measurements at selected temperatures

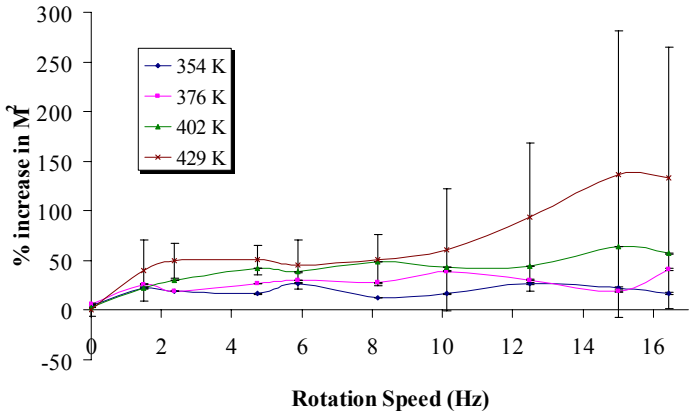

Figure 8: Variation of the normalized M^2 with SPGL rotation speed at chosen temperatures.

The other aberrations do not show particular trends and are generally very small. However, these are the aberrations that have the most effect on both beam quality and wavefront deformation. As can be observed in Figure 8, M^2 increases with pipe rotation rate and pipe wall temperature. This is hypothesised to be the result of the cumulative effect of all the high order aberrations where, as can be observed in Table 2, there is no single dominant one. This cumulative effect is coupled by the fact that M^2 is showing an increasing variance with rotation rate as shown by the error bars depicting variance in the data in Figure 8. This suggests an increase in the random mixing of gases at higher rotation rates and temperature, due to an increase in the unstable region near the wall of the pipe.

6. CONCLUSION

This study considered the effects of a spinning pipe gas lens on the wavefront of a laser beam. A computational fluid dynamics model of the gas mixing inside the SPGL was used to gain some insights into the gas mixing processes, and we are able to confirm numerically previously observations as to the lensing region of the pipe. Wavefront measurements on the laser beam after passing through the pipe have shown that although defocus is indeed evident as expected, higher order aberrations are measured together with a concomitant decrease in laser beam quality. The fact that the laser beam deteriorates as it passes through the SPGL is a new finding, and suggests that use of such a lens may be limited to those applications where poor beam quality is not an issue, or where sufficient power exists in the laser to create even more severe problems in conventional lenses, thus making the gas lens preferable.

REFERENCES

1. A. E. Siegman, "Laser Beams and Resonators: The 1960s", *IEEE Jour. of special topics in Quant. Elec.* 20(5), 100–108 (1999).
2. D. Marcuse, "Theory of a Thermal Gradient Gas Lens", *IEEE Trans. on Microwave Theory & Technology,* MMT-13(6), 734–739 (1965).
3. W. H. Steier, "Measurements on a Thermal Gradient Gas Lens", *IEEE Trans. on Microwave Theory & Technology,* MMT-13(6), 740–748 (1965).
4. D. Gloge, "Deformation of Gas Lenses by Gravity", *Bell Sys. Tech. Jour.*, 46(2) 357–365 (1967).
5. P. Kaiser, "Measured Beam Deformations in a Guide Made of Tubular Gas Lenses", *Bell Sys. Tech. Jour.,* 47 179–194 (1967).
6. Y. Aoki, M. Suzuki, "Imaging Property of a Gas Lens", *IEEE Trans. on Microwave Theory & Techniques*, 15(1), (1967).
7. A. K. Ghatak, D. P. S. Malik, I. C. Goyal, "Electromagnetic Wave Propagation Through a Gas Lens" *Jour. of Modern Optics*, 20(4), 303–312 (1973).
8. O. G. Martynenko, "Aerothemooptics" *International Jour. on Heat and Mass Transfer*, 18, 793–796 (1975).
9. M. M. Michaelis, M. Kuppen, A. Prause, A. Forbes, N. Viranna, N. Lisi, "Progress with Gas Lenses" *Laser & Particle Beams,* 14(3) 473–485 (1996)
10. M. M. Michaelis, A. Forbes, A. Conti, N. Nativel, H. Bencherif, R. Bingham, B. Kellet, K. Govender, "Non-solid, non-rigid optics for high power laser systems", *Pro. SPIE* 6261, (2006).
11. M. M. Michaelis, M. Notcutt, P. F. Cunningham, "Drilling by a Gas Lens Focused Laser", *Opt. Comm.*, 59, 369–374 (1986).
12. M. M. Michaelis, P. F. Cunningham, R. S. Cazalet, J. A. Waltham, M. Notcutt, "Gas Lens Applications", *Laser & Particle Beams,* 9(2), 641–651 (1991).
13. M. M. Michaelis, M. Notcutt, P. F. Cunningham, J. A. Waltham, "Spinning Pipe Gas Lens", *Optics and Laser Technology,* 20(5), 243–250 (1988).
14. A. Forbes, *Photothermal Refraction and Focusing*, PhD Thesis, University of Natal, (1997)
15. C. Mafusire, *Gas Lensing in a Heated Rotating Pipe*, MSc Thesis, University of Zimbabwe, (2006).
16. N. Lisi, R. Bucellato, M. M. Michaelis, "Optical quality and temperature profile of a spinning pipe gas lens", *Optics and Laser Technology,* 26, 25–27(1994).
17. M. Born, E.Wolf, *Principle of Optics,* Pergamon Press, (1999).
18. L. Davison, "An Introduction to Turbulence Models", *Chalmers University Of Technology* (2003), http://www.tfd.chalmers.se/~lada/postscript_files/kompendium_turb.pdf